632, 88, 0.9997. For the experiments in the presence of the alkaline earth bromides, the ϵ_{296} values of the associated forms were used. In all cases the concentration of the buffer components was $[Et_3N] = [Et_3NHBr] = 4 \times 10^{-2}$ M. A least-squares treatment of the data as above gave the following a and b values and correlation coefficients in the given order: Ca^{2+}, 4.69×10^5, 16, 0.9893; Sr^{2+}, 5.34×10^5, 73, 0.9994; Ba^{2+}, 7.78×10^5, 152, 0.9998.

Equilibrium measurements involving the cyclic ligand C were carried out by measuring the absorbance changes of a dilute (1.42×10^{-5}–1.05×10^{-4} M) solution of C upon addition of increasing amounts of metal bromide. In order to improve sensitivity a 40 mm cuvette was used and different wavelengths were chosen for the various salts. These were 267 nm for Na^+, 283 nm for K^+, 283 nm for Rb^+, 275 nm for Cs^+, 280 nm for Ca^{2+}, 280 nm for Sr^{2+}, and 234 nm for Ba^{2+}. A typical run is reported in Table V. The absorbance readings in each run were treated according to eq 7 by a least-squares procedure. Two independent sets of measurements were carried out for the alkali bromides. In the case of the alkaline earth bromides a second set of experiments was carried out in the presence of the 0.04 M triethylamine–triethylammonium bromide buffer in order to demonstrate the lack of substantial interactions of the alkaline earth cations with the buffer components (see Results section). Log K_C values reported in Table I refer only to measurements carried out in the absence of buffer. For each cation K_C values and correlation coefficients are given in that order—data in parentheses refer to equilibrium measurements in the presence of the buffer: Na, 1.18×10^4, 0.9991; 0.97×10^4, 0.9969; K^+, 2.15×10^5, 0.9980; 1.56×10^5, 0.9893; Rb^+, 4.25×10^4, 0.9988; 4.07×10^4, 0.9906; Cs^+, 4.21×10^3, 0.9974; 4.93×10^3, 0.9927; Ca^{2+}, 3.13×10^3, 0.9942; (3.43×10^3, 0.9919); Sr^{2+}, 8.23×10^4, 0.9983; (6.58×10^4, 0.9928); Ba^{2+}, 2.25×10^5, 0.9981; (1.48×10^5, 0.9884).

Homogeneous Catalysis of the Electrochemical Reduction of Dioxygen by a Macrocyclic Cobalt(III) Complex

Thomas Geiger and Fred C. Anson*

Contribution No. 6432 from the Division of Chemistry and Chemical Engineering, Arthur Amos Noyes Laboratories, California Institute of Technology, Pasadena, California 91125.
Received May 11, 1981

Abstract: The rotating ring–disk electrode was used to examine the reduction of dioxygen to hydrogen peroxide as catalyzed by the macrocyclic cobalt complex, *trans*-$[Co([14]aneN_4)(OH_2)_2]^{3+}$. Two different mechanisms were identified that depended on the ratio of dioxygen to cobalt. With excess cobalt, a well-characterized μ-peroxo complex, *trans*-$[(Co([14]aneN_4)(OH_2))_2O_2]^{4+}$, is formed at potentials where the initial Co(III) complex is reduced. At more negative potentials the μ-peroxo complex is reduced to H_2O_2 and $[Co([14]aneN_4)(OH_2)_2]^{2+}$ which re-enters the catalytic cycle. With excess dioxygen, the initial product of the reaction between the Co(II) complex and dioxygen is very rapidly further reduced to form a new complex thought to be *trans*-$[Co([14]aneN_4)(OH_2)(O_2H)]^{2+}$, a new, end-bonded, hydroperoxide complex. The hydroperoxide complex is further reduced at more negative potentials to yield H_2O_2 and $[Co([14]aneN_4)(OH_2)_2]^{2+}$. The rate of reaction of $[Co([14]aneN_4)(OH_2)_2]^{2+}$ with dioxygen proved too fast to measure with the rotating ring–disk electrode. The related complex, $[Co(Me_6[14]4,11\text{-diene } N_4)(OH_2)_2]^{3+}$, also catalyzes the reduction of dioxygen and at a much more positive potential but at a somewhat lower rate.

Several reports in the recent literature have described the use of transition-metal complexes as catalysts for the electrochemical reduction of dioxygen.[1-5] Among the goals of such studies is the development of catalysts that function at graphite or other inexpensive electrodes while approaching (or, conceivably, even exceeding) the catalytic activity of the platinum cathodes presently utilized in fuel cells. The use of catalysts that are confined to electrode surfaces has much to recommend it[1-5] but there are associated difficulties in carrying out kinetic and mechanistic studies with such small quantities of catalysts. The concentrations of catalyst present on the surface are often not known precisely and instability of catalyst coatings can introduce added uncertainties.

In recent studies of the catalytic activity of a highly active, dimeric cofacial porphyrin complex of cobalt(II) attached to graphite electrodes it was argued that a key intermediate in the catalytic mechanism is a peroxo-bridged dicobalt(III) complex.[5] Detailed information on the electrochemical behavior of such species is lacking and we sought to learn more about the properties and electrochemical reactivity of this class of reactants by studying some examples based on water-soluble macrocyclic complexes. We began with the cobalt(III) complex of 1,4,8,11-tetraazacyclotetradecane, $[Co([14]aneN_4)(OH_2)_2]^{3+}$,[6] because it has been well characterized,[7] its redox chemistry has been explored,[8] and the cobalt(II) complex is known to exhibit a high reactivity toward dioxygen.[9]

A particularly attractive feature of this complex was the recent demonstration by Endicott and co-workers[9b] that its reaction with dioxygen leads to the formation of a binuclear μ-peroxo-bridged complex with a structure rather similar to that proposed by Collman et al.[5] It is of interest to determine the factors that affect

(1) (a) H. Behret, W. Clauberg, and G. Sandstede, *Ber. Bunsenges. Phys. Chem.*, **81**, 54–60 (1977); (b) H. Behret, W. Clauberg, and G. Sandstede, *ibid.*, **83**, 139–147 (1979); (c) H. Behret, W. Clauberg, and G. Sandstede, *Z. Phys. Chem. (Wiesbaden)*, **113**, 97–116 (1978).

(2) (a) J. Zagal, P. Bindra, and E. Yeager, *J. Electrochem. Soc.*, **127**, 1506–1517 (1980); (b) J. Zagal, R. Y. Sen, and E. Yeager, *ibid.*, **83**, 207–213 (1977).

(3) (a) A. Bettelheim and T. Kuwana, *Anal. Chem.*, **51**, 2257–2260 (1979); (b) A. Bettelheim, R. J. H. Chan, and T. Kuwana, *J. Electroanal. Chem.*, **110**, 93–102 (1980).

(4) A. J. Appelby and M. Savy, *Electrochim. Acta*, **21**, 567–574 (1976).

(5) J. P. Collman, P. Denisevich, Y. Konai, M. Marrocco, C. Koval, and F. C. Anson, *J. Am. Chem. Soc.*, **102**, 6027–6036 (1980).

(6) Ligand abbreviations are based on conventions described by G. A. Melson in "Chemistry of Macrocyclic Compounds", G. A. Melson, Ed., Plenum Press, New York, 1979, Chapter 1, p 1.

(7) B. Bosnich, C. K. Poon, and M. L. Tobe, *Inorg. Chem.*, 4, 1102–1108 (1965).

(8) J. F. Endicott and B. Durham in "Chemistry of Macrocyclic Compounds", G. A. Melson, Ed., Plenum Press, New York, 1979, Chapter 6, p 415 ff.

(9) (a) G. McLendon and M. Mason, *Inorg. Chem.*, **17**, 362–365 (1978). (b) C. L. Wong, J. A. Switzer, B. P. Balakrishnan, and J. F. Endicott, *J. Am. Chem. Soc.*, **102**, 5511–5518 (1980).

0002-7863/81/1503-7489$01.25/0

the reactivity of such μ-peroxo-bridged complexes toward further reduction.

Most of the experiments to be described were carried out with a rotating ring–disk electrode composed of a graphite disk and a concentric platinum ring.[10] The utility of such electrodes in examining the catalyzed reduction of dioxygen is well known[10] and was exemplified in the recent study of a dicobalt cofacial porphyrin catalyst.[5] In the present experiments the catalytically active complex, $[Co([14]aneN_4)(OH_2)_2]^{2+}$, is generated at the disk electrode in solutions containing both dioxygen and the cobalt(III) precursor complex. The reactions that these two engage in as they are swept across the insulating gap separating the disk and ring electrodes can be discerned from the resulting electrochemical responses observed at the ring electrode. In this way two different reaction pathways were uncovered and the formation of what we believe to be a new mononuclear hydroperoxide complex of cobalt(III) was detected along one pathway.

Experimental Section

Preparation of Complexes and Solutions. Literature procedures were employed for the synthesis of *trans*-$[Co([14]aneN_4)(Cl)_2]Cl$[7] and *trans*-$[Co([14]aneN_4)(OH_2))_2O_2](ClO_4)_4$[11] where "[14]aneN$_4$" stands for 1.4.8.11-tetraazacyclotetradecane.[6] The ligand was from Strem

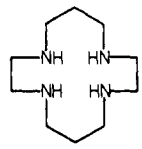

Chemical Co. Solutions of *trans*-$[Co([14]aneN_4)(OH_2)_2]^{3+}$ were prepared by base hydrolysis of *trans*-$[Co([14]aneN_4)(Cl)_2]^+$ followed by acidification with perchloric acid. The resulting green solution was loaded on an anion exchange column (Bio Rad AG 1-X2, 200–400 mesh. perchlorate form) and eluted with 0.5 M perchloric acid to obtain a chloride-free solution.[12] Solutions were prepared from reagent grade 60% perchloric acid and distilled water that had been further purified by passage through a commercial purification train (Barnstead Nanopure). Electronic spectra of solutions of the complexes (obtained with a Hewlett Packard Model 8450 spectrometer) matched those reported in previous studies.[7,11,12]

Electrochemistry. Most measurements were conducted with rotating disk and ring–disk electrodes according to conventional practice.[10] The ring–disk electrode. electrode rotator, and the bipotentiostat were from Pine Instrument Co. (Grove City. Pa.). An x–y–y' recorder (Hewlett Packard Model 7046) was used to record disk and ring current–potential curves simultaneously. A single compartment cell was employed with a platinum wire auxiliary electrode. The reference electrode was separated from the main cell compartment by immersion in a glass tube terminated by a sintered glass frit.

The radius of the disk electrode was 0.382 cm (A = 0.46 cm^2). The inner and outer ring radii were 0.399 and 0.422 cm. respectively. The collection efficiency[10] (measured by reducing $[Fe(CN)_6]^{3-}$ at the disk and oxidizing the resulting $[Fe(CN)_6]^{4-}$ at the ring) was 0.175 in good agreement with the value calculated from the electrode geometry.[14]

Measurements at the highest rotation rates were difficult with the commercial electrode because of turbulence and bubble formation in our relatively small cell (150 cm^3). For these experiments a rotating disk electrode having a smaller-diameter sheath was made by sealing an edge plane pyrolytic graphite disk with an area of 0.34 cm^2 to a stainless steel tube with heat-shrinkable tubing. The steel tube was connected to a shaft that was machined to fit the commercial electrode rotator.

Pyrolytic graphite electrodes were polished with an aqueous suspension of 0.3 μm alumina on a polishing cloth before each scan and occasionally on silicon carbide 600 paper. In addition, the platinum ring electrode was pretreated electrochemically: While rotating the electrode in deaerated 0.5 M perchloric acid the ring electrode was oxidized at +1.6 V for ca. 3 min and then reduced at −0.3 V for an additional 3 min. This procedure was repeated twice and the electrodes were finally held at +0.2 V for 2 min.[15]

Experiments were conducted at ambient temperature. 22 ± 2 °C. Potentials were measured and are quoted with respect to a sodium chloride-saturated calomel electrode (SSCE).

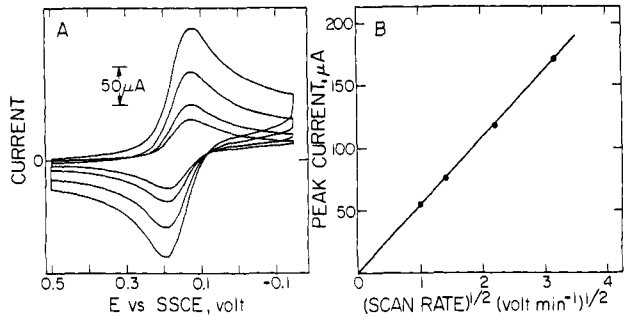

Figure 1. (A) Cyclic voltammograms for 1.5 mM $[Co([14]aneN_4)(OH_2)_2]^{3+}$ at a pyrolytic graphite electrode. Supporting electrolyte: 0.5 M $HClO_4$. Scan rates: 1. 2. 5 and 10 V min^{-1}. (B) Cathodic peak current vs. (scan rate)$^{1/2}$ for the voltammograms in part A.

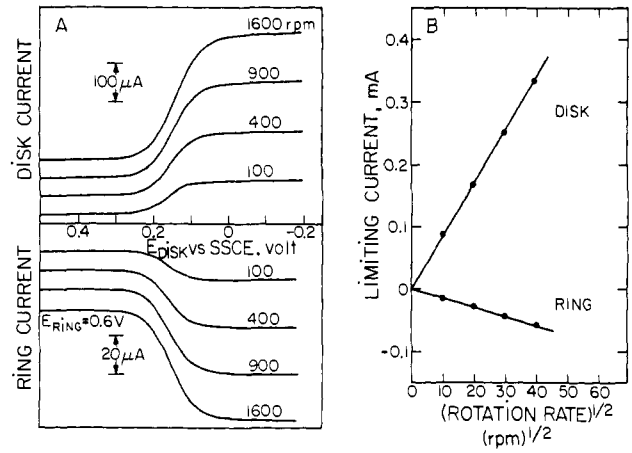

Figure 2. (A) Ring–disk current–potential curves for the solution from Figure 1 at a rotating graphite disk–platinum ring electrode. Electrode rotation rates: 100, 400. 900, 1600 rpm. Ring potential: +0.6 V. Disk currents are cathodic; ring currents are anodic. (B) Plots of the limiting disk and ring currents vs. (rotation rate)$^{1/2}$.[13]

Results

Electrochemistry of *trans*-$[Co([14]aneN_4)(OH_2)_2]^{3+}$ in the Absence of Dioxygen. The cyclic voltammetry of $[Co([14]aneN_4)(OH_2)_2]^{3+}$ in carefully deaerated supporting electrolyte is illustrated in Figure 1A. The separation between cathodic and anodic peaks increases with scan rate suggesting that the electrode reaction is not perfectly nernstian but the equality of peak currents shows the reaction to be reversible. The peak currents increase linearly with (scan rate)$^{1/2}$ (Figure 1B) showing the reaction to be diffusion controlled. The average of the cathodic and anodic peak potentials gives a formal potential of 0.16 V vs. SSCE which is quite close to the value (0.42 V vs. NHE) quoted by Endicott et al.[9b]

Figure 2A shows the current–potential responses obtained at the rotating ring–disk electrode in the absence of dioxygen. The ratio of ring to disk currents matched the values measured in independent experiments with $[Fe(CN)_6]^{3-}$ or $[Ru(NH_3)_6]^{3+}$ at all rotation rates studied (Figure 2B), confirming the stability of the $[Co([14]aneN_4)(OH_2)_2]^{2+}$ complex in the absence of dioxygen. The diffusion coefficient for $[Co([14]aneN_4)(OH_2)_2]^{3+}$ evaluated

(10) W. J. Albery and M. L. Hitchman. "Ring Disc Electrodes". Clarendon Press. Oxford. 1971.

(11) B. Bosnich. C. K. Poon, and M. L. Tobe. *Inorg. Chem.*. **5**. 1514–1517 (1966).

(12) We thank Professor John Endicott for helpful comments concerning the preparation and for the electronic spectrum of *trans*-$[Co([14]aneN_4)(OH_2)_2]^{3+}$.

(13) V. G. Levich. "Physicochemical Hydrodynamics". Prentice Hall. Englewood Cliffs. N.J., 1962.

(14) W. J. Albery and S. Bruckenstein. *Trans. Faraday Soc.*. **62**. 1920–1931 (1966).

(15) We found that the current response of the platinum ring electrode to hydrogen peroxide (generated by a disk electrode reaction) was strongly influenced by its pretreatment in our solutions. Not infrequently collection efficiencies for H_2O_2 were 10–25% below that for simple redox couples such as $Fe(CN)_6^{3-/4-}$.

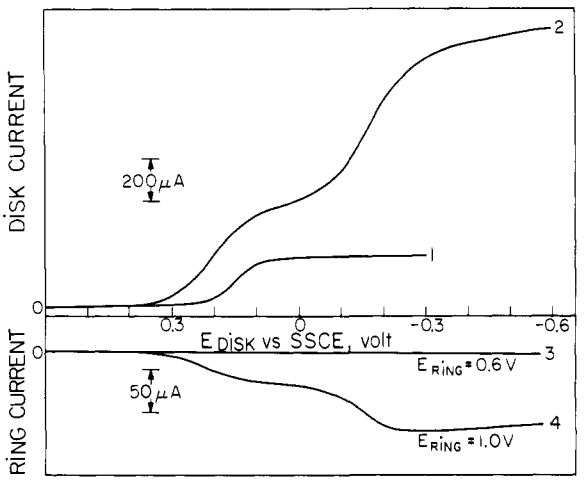

Figure 3. Ring–disk current–potential curves for 1.5 mM $[Co([14]aneN_4)(OH_2)_2]^{3+}$ in 0.5 M $HClO_4$ at a rotation rate of 900 rpm. (Curve 1) Disk current in the absence of dioxygen. (Curve 2) Disk current in dioxygen-saturated solution. (Curve 3) Ring current vs. disk potential in dioxygen-saturated solution with ring potential at 0.6 V. (Curve 4) As in 3 except ring potential is at 1.0 V.

from the limiting disk currents was 5×10^{-6} cm^2 s^{-1}.

Rotating Ring–Disk Measurements in the Presence of Dioxygen. The responses obtained at rotating ring–disk electrodes during the reduction of $[Co([14]aneN_4)(OH_2)_2]^{3+}$ in the presence of dioxygen depend upon which reactant is present in excess. Since the two reactants are brought together in the "Levich layer"[13] present at the surface of the rotated electrode, it is the relative fluxes rather than the concentrations of the two reactants that determine the course of the reaction.[16] At rotating disk electrodes the flux of a reactant is proportional to the product $D^{2/3}C^b$ where D is the diffusion coefficient and C^b the bulk concentration of the reactant. The diffusion coefficient of dioxygen, 1.8×10^{-5} cm^2 s^{-1},[17] is considerably larger than that of $[Co([14]aneN_4)(OH_2)_2]^{3+}$, 5×10^{-6} cm^2 s^{-1}, so that equal fluxes of the two reactants result when the ratio of their concentrations is 2.3. The concentration of dioxygen in a solution saturated at 1 atm and 22 °C is 1.4 mM[18] so that the dioxygen flux at the electrode will exceed that of the cobalt complex at concentrations of the latter below 3.2 mM.

A current–potential curve for the reduction of $[Co([14]aneN_4)(OH_2)_2]^{3+}$ at a rotating disk electrode in the presence of excess dioxygen is shown as curve 2 in Figure 3. Two stages of reduction are evident. The first reduction wave appears at a potential about 100 mV more positive than that for the complex alone. Such a positive potential shift is expected whenever the product of an electroreduction is consumed rapidly in a chemical reaction that follows the electrode reaction.[19] During the recording of the disk current–potential curve no current is observed at the platinum ring electrode maintained at +0.6 V (curve 3) where $[Co([14]aneN_4)(OH_2)_2]^{2+}$ is oxidized (Figure 3). This was true at all accessible rotation rates and confirms that the cobalt(II) complex is completely consumed by reaction with dioxygen during the time required for its convective transfer from the disk to the ring electrode.

The products formed at the disk electrode on both the first and second waves are evidently oxidizable at the ring electrode when its potential is adjusted to 1.0 V (Figure 3, curve 4). Hydrogen peroxide is one possible product that would behave in this way but another oxidizable product is also present as will be shown below. The current on the plateau of the first wave of curve 2 is approximately twice as large as the limiting current for the one-electron reduction of $[Co([14]aneN_4)(OH_2)_2]^{3+}$ in the absence of dioxygen (curve 1) and remains independent of changes in the concentration of dioxygen in the solution until the flux of dioxygen reaching the electrode exceeds the flux of $[Co([14]aneN_4)(OH_2)_2]^{3+}$.

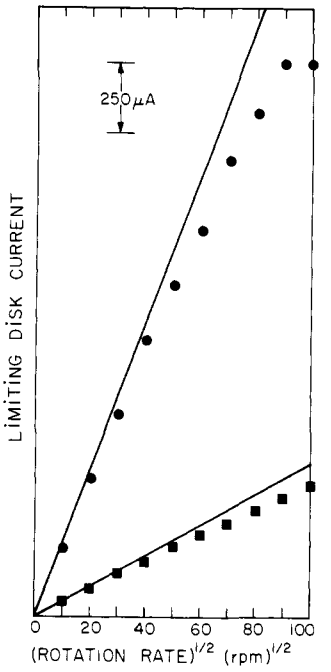

Figure 4. Levich plots of limiting disk currents vs. (rotation rate)$^{1/2}$ for the second wave in Figure 3 with 0.03 mM $[Co([14]aneN_4)(OH_2)_2]^{3+}$. Solution saturated with dioxygen (●) or air (■). The lines give the calculated Levich currents for the sum of a one-electron reduction of the cobalt complex and a two-electron reduction of dioxygen.

The half-wave potentials for curve 1 and for the first wave in curve 2 are independent of pH between pH 0 and 3 showing that no protonation steps accompany or precede the electron transfer to cobalt(III) whether or not dioxygen is present. The half-wave potential of the second wave in curve 2 shifts to more positive values as the pH is decreased by about 60 mV per pH unit.

At low and intermediate electrode rotation rates the current measured on the plateau of the second wave in curve 2 of Figure 3 matches that expected for the combination of a one-electron reduction of $[Co([14]aneN_4)(OH_2)_2]^{3+}$ and a two-electron reduction of dioxygen. However, at higher rotation rates the current falls below the extrapolated line as shown in the Levich plots[13] in Figure 4. Such deviations could result from the onset of kinetic limitations in the chemical reactions responsible for the catalyzed electrode reaction.[10] However, even larger relative deviations would then be expected at lower reactant concentrations if the limiting reaction were second order. In fact, smaller deviations are observed when air-saturated solutions are substituted for dioxygen-saturated solutions (Figure 4) and the deviations were virtually independent of the concentration of the cobalt complex between 0.03 and 1 mM. Thus, the behavior obtained in dioxygen-saturated solutions is not attributable to kinetic limitations originating in the chemical reactions responsible for the catalysis. The same conclusion follows from our failure to detect unreacted $[Co([14]aneN_4)(OH_2)_2]^{2+}$ at the ring electrode at rotation rates where deviations from linearity appear in the Levich plots. The deviations from linearity of the upper Levich plot in Figure 4 at high rotation rates may result from air being swept into the solution (despite the cover on the cell) so that the solution becomes less than saturated with respect to dioxygen at one atmosphere. The smaller deviations in the lower Levich plot must have a different origin which we did not identify.

In order to identify all of the products resulting from the reduction of $[Co([14]aneN_4)(OH_2)_2]^{3+}$ in the presence of dioxygen it is useful to maintain the rotating disk electrode at a fixed

(16) W. J. Albery, S. Bruckenstein, and D. C. Johnson, *Trans. Faraday Soc.*, **62**, 1938–1945 (1966).
(17) K. Grubbins and R. Walker, *J. Electrochem. Soc.*, **112**, 469–471 (1965).
(18) W. F. Linke, "Solubilities of Inorganic and Metallorganic Compounds", Vol. 11, 4th ed., American Chemical Society, Washington, D.C., 1965, p 1229.
(19) A. J. Bard and L. R. Faulkner, "Electrochemical Methods, Fundamentals and Applications", J. Wiley and Sons, New York, 1980, Chapter 11.

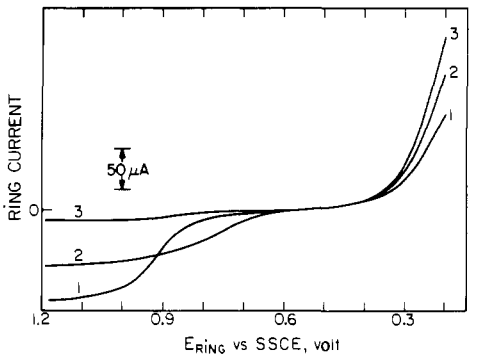

Figure 5. Rotating ring–disk measurements at fixed disk potentials with the potential of the ring electrode scanned. 1.5 mM $[Co([14]aneN_4)(OH_2)_2]^{3+}$ in 0.5 M $HClO_4$ saturated with dioxygen. Graphite disk potentials were: (curve 1) −0.40 V; (curve 2) 0.05 V: (curve 3) disk disconnected. The steady disk currents were: 1250 and 500 μA at −0.40 and 0.05 V, respectively. The potential of the platinum ring was scanned at 500 mV min^{-1}. Electrode rotation rate was 900 rpm.

potential while varying the potential of the ring. Figure 5 shows the results of such experiments with the disk maintained at +0.05 V (first plateau) or −0.40 V (second plateau in Figure 3) or with the disk disconnected from the potentiostat. At potentials more negative than ca. 0.40 V the direct reduction of dioxygen commences at the platinum ring electrode and blends with the reduction of $[Co([14]aneN_4)(OH_2)_2]^{3+}$ that begins near 0.2 V. The magnitude of the ring current at potentials negative of 0.40 V diminishes as the disk potential is changed from open circuit to 0.05 V to −0.40 V because the fluxes of oxygen and $[Co([14]aneN_4)(OH_2)_2]^{3+}$ reaching the ring decrease as the fraction of each reactant that is reduced at the disk instead of the ring increases. No ring current flows at potentials positive of 0.40 V with the disk at open circuit (curve 3, Figure 5) because no reaction products are being formed at the disk. With the disk at −0.40 V (curve 1) an anodic wave appears at the ring electrode with a half-wave potential, +0.9 V, characteristic of the oxidation of hydrogen peroxide which is evidently the only oxidizable product formed at the disk at −0.40 V. (The collection efficiency of the ring electrode for the oxidation of hydrogen peroxide was somewhat variable in these solutions and rarely exceeded 70 to 80% of the value expected if the disk current at −0.40 V in excess of that corresponding to the reduction of $[Co([14]aneN_4)(OH_2)_2]^{3+}$ was attributed to the exclusive production of H_2O_2. We have assumed that this discrepancy results from some hydrogen peroxide escaping oxidation at the ring rather than from the formation of a second, unoxidizable reaction product at the disk.)

When the disk potential is maintained at 0.05 V (curve 2, Figure 5), hydrogen peroxide no longer appears at the ring as evidenced by the absence of an oxidation wave at +0.9 V. However, an oxidizable product of the disk reaction is detected at the ring with a half-wave potential of ca. 0.8 V. The ratio of ring current at, say, 1.0 V to the disk current (at 0.05 V) is quite close to the measured collection efficiency of the electrode showing that the same number of electrons is involved in the disk and ring reactions under the conditions used to record curve 2.

Controlled Potential Electrolyses. In order to gain more information on the nature of the reaction products, the reduction of $[Co([14]aneN_4)(OH_2)_2]^{3+}$ in dioxygen-saturated solution was carried out at controlled potential, using the rotating graphite disk as the working electrode and isolating the platinum auxiliary electrode from the main cell compartment by two sintered glass frits. If the rotating disk was maintained at −0.5 V while dioxygen was continuously bubbled into the solution, steady disk currents were obtained that did not decrease with time. The spectrum of the solution also remained invariant during the electrolysis (Figure 6A). After approximately two electrons per molecule of $[Co([14]aneN_4)(OH_2)_2]^{3+}$ had passed through the solution, hydrogen peroxide was easily detected in the solution by anodic voltammetry with a platinum electrode. The behavior was entirely consistent with the complex cycling between cobalt(III) and cobalt(II) while

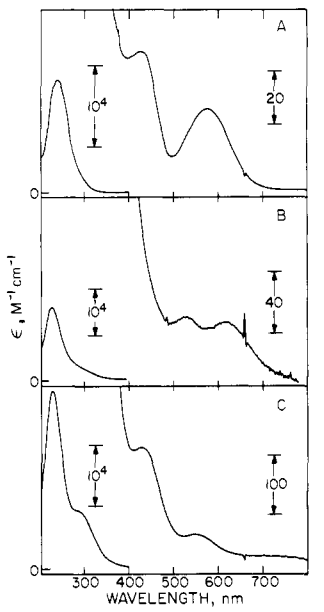

Figure 6. Spectra of some of the complexes studied in 0.5 $MHClO_4$: (A) *trans*-$[Co([14]aneN_4)(OH_2)_2]^{3+}$: (B) After the solution from A was reduced at +0.05 V in dioxygen-saturated solution where 1.9 electrons per cobalt were consumed: (C) *trans*-$[(Co([14]aneN_4)(OH_2))_2O_2]^{4+}$.

serving as an efficient redox catalyst for the reduction of dioxygen to hydrogen peroxide as had been indicated from the ring–disk voltammetry shown in Figures 3 and 5.

When the controlled potential electrolysis was repeated with the disk potential maintained at 0.05 V, the current decayed continuously during the electrolysis indicating that the cobalt complex was being consumed. The current dropped to about 10% of its initial value after 1.9 electrons per molecule of $[Co([14]aneN_4)(OH_2)_2]^{3+}$ had been consumed and the spectrum of the solution changed significantly (Figure 6B). Dioxygen was removed from the electrolyzed solution and it was inspected by cyclic voltammetry. An oxidation wave was present at +0.77 V (peak potential) and a reduction wave at −0.1 V. The voltammogram showed no evidence of hydrogen peroxide. Speculation on the identity of the species responsible for the electrochemical responses will be deferred to the Discussion section.

Reduction of *trans*-$[Co([14]aneN_4)(OH_2)_2]^{3+}$ in the Absence of Excess Dioxygen. The reduction of $[Co([14]aneN_4)(OH_2)_2]^{3+}$ at concentrations large enough so that the flux of the complex at the rotating disk electrode exceeds that of dioxygen leads to different electrochemical responses at the rotating ring and disk electrodes. Figure 7A presents a set of ring–disk current–potential curves recorded under these conditions. Curve 1 is the disk current for the reduction of the cobalt complex in the absence of dioxygen. Curve 2 results when the solution is saturated with air (instead of dioxygen in order to provide a high ratio of the cobalt to dioxygen fluxes). Three reduction waves are present with the second appearing at the potential characteristic of the reduction of $[Co([14]aneN_4)(OH_2)_2]^{3+}$ in the absence of dioxygen. The total current on the plateau of the second wave remains independent of the concentration of dioxygen so long as the reactant concentrations are such that the flux of the complex is at least twice as great as that of dioxygen. The limiting current on the third plateau of curve 2 remains equal to the sum of the calculated Levich currents for the one-electron reduction of all of the complex present and the two-electron reduction of dioxygen, just as was true under the conditions of Figure 3. The current on the first plateau of curve 2 in Figure 7A is essentially equal to the difference in currents on the second and third plateaus. It represents the net increase in total current produced by the addition of dioxygen to the solution.

The first and second waves are clearly due to the reduction of $[Co([14]aneN_4)(OH_2)_2]^{3+}$ in the presence and absence of oxygen, respectively. The first wave appears at more positive potentials

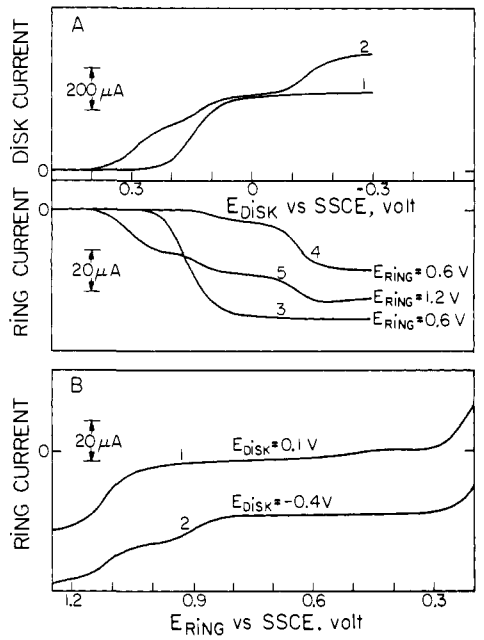

Figure 7. Rotating ring–disk responses for 2.2 mM $[Co([14]aneN_4)(OH_2)_2]^{3+}$ in air-saturated 0.5 M $HClO_4$. Rotation rate: 900 rpm. (The flux of cobalt complex at the disk is 3.4 times the flux of dioxygen.) (A) Disk current–potential curves and corresponding ring current–disk potential curves. (Curves 1 and 3) Disk and ring currents in deaerated electrolyte, ring potential 0.6 V; (curves 2 and 4) disk and ring currents in air-saturated electrolyte, ring potential +0.6 V; (curve 5) ring current with ring potential at +1.2 V. (B) Current–potential response at the ring electrode with the disk electrode maintained at a constant potential: (curve 1) disk electrode potential, 0.1 V, (curve 2) disk electrode potential, −0.4 V. The steady disk currents were 0.3 and 0.6 mA at 0.1 and −0.4 V, respectively.

as expected if the $[Co([14]aneN_4)(OH_2)_2]^{2+}$ product were rapidly consumed in a chemical reaction succeeding the electrode reaction.[19] The second wave, appearing at the same potential as in curve 1, represents the reduction of the $[Co([14]aneN_4)(OH_2)_2]^{3+}$ that is present in excess of dioxygen. The $[Co([14]aneN_4)(OH_2)_2]^{2+}$ resulting from its reduction is not rapidly consumed by reaction with dioxygen so the wave appears at its usual potential.

This interpretation is reinforced by the simultaneous responses obtained at the ring as shown in curves 3, 4, and 5 of Figure 7A. Curve 3 shows the expected simple ring response corresponding to reoxidation of the $[Co([14]aneN_4)(OH_2)_2]^{2+}$ that is generated at the disk and transported to ring in the absence of dioxygen. Curve 4 shows that the product of the reduction at the disk on the first wave in curve 2 is not oxidizable at the ring at +0.6 V, as expected if the $[Co([14]aneN_4)(OH_2)_2]^{2+}$ generated at the disk reacts with dioxygen before it can reach the ring. No ring current appears until the disk reaches the potential where the excess $[Co([14]aneN_4)(OH_2)_2]^{3+}$ is reduced and the resulting cobalt(II) complex can be carried to the ring because all of the dioxygen it would otherwise encounter has been consumed by reaction with the cobalt(II) complex generated on the first wave. The additional ring response as the disk potential reaches the third wave of curve 2 indicates that additional $[Co([14]aneN_4)(OH_2)_2]^{2+}$ is generated at these potentials. Curve 5 shows that the product of the disk reaction on the first wave of curve 2 is oxidizable at a ring potential of 1.2 V. The second and third waves in curve 5 have the same origin as they did in curve 4.

More information as to the properties of the reaction products originating at the disk electrode under the conditions of Figure 7A can be extracted from the current–potential curves for the ring electrode shown in Figure 7B with the disk electrode held at a fixed potential. With the disk potential at 0.1 V (i.e., near the plateau of the second wave in curve 2 of Figure 7A), essentially no ring response is observed at potentials between 0.3 and 1.05 V. This demonstrates that hydrogen peroxide is not produced at

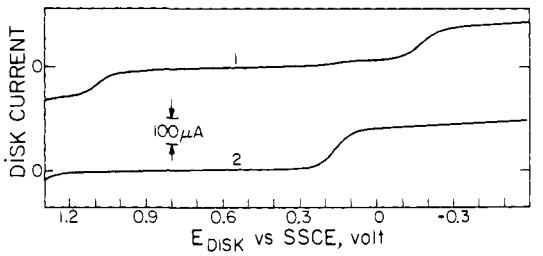

Figure 8. Current–potential curves for 0.5 mM $[(Co([14]aneN_4)(OH_2))_2O_2]^{4+}$ at a rotating graphite disk electrode. Supporting electrolyte: deaerated 0.5 M $HClO_4$. Electrode rotation rate: 1600 rpm. (Curve 1) Freshly prepared solution. (Curve 2) After 1 week.

the disk at 0.1 V. However, the anodic ring current obtained at more positive potentials shows that the product of the disk reaction can be oxidized at ca. 1.1 V. With the disk at −0.4 V (on the plateau of the third wave in curve 2 of Figure 7A), hydrogen peroxide is detected at the ring (in the form of the oxidation wave at 0.9 V) as well as the species that is oxidizable at 1.1 V. The latter was identified as the μ-peroxocobalt(III) complex, $[(Co([14]aneN_4)(OH_2))_2O_2]^{4+}$, by comparison with the electrochemistry of a solution of this species synthesized independently.

Electrochemistry of *trans*-$[(Co([14]aneN_4)(OH_2))_2O_2]^{4+}$. When $[Co([14]aneN_4)(OH_2)_2]^{3+}$ is reduced in the presence of less than an equivalent flux of dioxygen the most likely product is the μ-peroxo dimer, $[(Co([14]aneN_4)(OH_2))_2O_2]^{4+}$, that Endicott et al. identified as the stable reaction product formed when excess $[Co([14]aneN_4)(OH_2)_2]^{2+}$ is mixed with dioxygen.[9b] The electrochemistry of this dimeric complex at the rotating disk electrode is shown in Figure 8. The complex exhibits both an oxidation and a reduction wave that are widely separated. The oxidation wave appears at +1.1 V with a limiting current corresponding to a one-electron process so that the wave probably represents the formation of the μ-superoxo complex.[20,21] The important point for diagnostic purposes is that the oxidation wave matches the wave at +1.1 V observed at the ring electrode in Figure 7B. The reduction wave at −0.15 V corresponds to two electrons per molecule of complex. In accord with this, rotating ring–disk measurements showed the reduction products to be $[Co([14]aneN_4)(OH_2)_2]^{2+}$ and H_2O_2.

$[(Co([14]aneN_4)(OH_2))_2O_2]^{4+}$ is known to undergo slow thermal decomposition in acidic electrolytes to yield $[Co([14]aneN_4)(OH_2)_2]^{3+}$,[11] among other products.[22] The very small wave near +0.5 V in Figure 8 reveals the presence of a trace of $[Co([14]aneN_4)(OH_2)_2]^{3+}$ and shows that some decomposition had proceeded in the solution used to obtain the current–potential curve. In experiments where the decomposition was monitored electrochemically with a rotating platinum disk electrode in 0.5 M $HClO_4$ we detected the release of much less H_2O_2 than of $[Co([14]aneN_4)(OH_2)_2]^{3+}$ during the decoposition. The reactions responsible for the decomposition are apparently complex but they can lead to a simple result. Thus, a fully decomposed solution produced both a spectrum and a current–potential response (curve 2, Figure 8) indicating essentially quantitative conversion to $[Co([14]aneN_4)(OH_2)_2]^{3+}$.

Discussion

One of our initial objectives was to compare the reduction of dioxygen as catalyzed by a cobalt macrocyclic complex dissolved in homogeneous solution with the reduction catalyzed by insoluble cobalt porphyrin complexes attached to the electrode surface.[5] By using the ring–disk electrode it was possible to demonstrate that the catalysts by $[Co([14]aneN_4)(OH_2)_2]^{2+}$ involves reaction between the complex and dioxygen in homogeneous solution because the intermediates generated (or consumed) can be detected by their responses (or absence of response) at the ring electrode. Thus, even if the reduction could proceed, in part, by a pathway

(20) G. McLendon and W. F. Mooney, *Inorg. Chem.*, **19**, 12–15 (1980).
(21) A. G. Sykes and J. A. Weil, *Progr. Inorg. Chem.*, **13**, 1–107 (1963).
(22) C.-L. Wong and J. F. Endicott, *Inorg. Chem.*, **20**, 2233–2239 (1981).

Table I. Electrode Processes Encountered in this Study (0.5 M $HClO_4$ Supporting Electrolyte)

electrode reaction	$E_{1/2}$ V vs. SSCE	notes
$[Co([14]aneN_4)(OH_2)_2]^{3+} + e^- \rightleftarrows [Co([14]aneN_4)(OH_2)_2]^{2+}$	0.16	*a*
$[(Co([14]aneN_4)(OH_2))_2O_2]^{4+} + 2e^- + 2H^+ \rightarrow 2[Co([14]aneN_4)(OH_2)_2]^{2+} + H_2O_2$	−0.15	*b–d*
$[(Co([14]aneN_4)(OH_2))_2O_2]^{4+} - e^- \rightarrow [(Co([14]aneN_4)(OH_2))_2O_2]^{5+}$	1.1	*b, d, e*
$[Co([14]aneN_4)(OH_2)(O_2H)]^{2+} + e^- + H^+ \rightarrow [Co([14]aneN_4)(OH_2)_2]^{2+} + H_2O_2$	−0.2	*b, c*
$[Co([14]aneN_4)(OH_2)(O_2H)]^{2+} - 2e^- \rightarrow [Co([14]aneN_4)(OH_2)_2]^{3+} + O_2 + H^+$	0.77	*b, d, e*
$[Co(Me_6[14]4.11\text{-diene }N_4)(OH_2)_2]^{3+} + e^- \rightleftarrows [Co(Me_6[14]4.11\text{-diene }N_4)(OH_2)_2]^{2+}$	0.32	*a*
$H_2O_2 - 2e^- \rightarrow O_2 + 2H^+$	0.9	*b, d*

[a] Reversible couple observed. [b] Irreverisible process. [c] Measured at graphite disk. [d] Measured at platinum ring. [e] Stoichiometry surmised from current magnitude but not demonstrated.

involving $[Co([14]aneN_4)(OH_2)_2]^{2+}$ adsorbed on the electrode (and we obtained no evidence for such a pathway), the portion of the reaction proceeding entirely by a pathway involving homogeneous catalyst and intermediates can be discerned unambiguously from the ring–disk current–potential behavior. This ability to discriminate between heterogeneous and homogeneous catalytic reaction pathways is one of the unique attributes of rotating ring–disk electrodes and was one of the reasons for the extensive use of this electrode system in this study.

The variety of electrochemical responses encountered in this study for both the initial reactants and the generated intermediates are summarized in Table I. All but two of the electrode processes in the table proceeded irreversibly so that the potentials listed are designed only for diagnostic purposes.

Electrode Processes with Excess Cobalt Complex. The course of the reaction between electrogenerated $[Co([14]aneN_4)(OH_2)_2]^{2+}$ and dioxygen depends on the molar ratio at which the two reactants encounter each other. With cobalt in sufficient excess the binuclear μ-peroxo-bridged cobalt(III) complex is formed in accord with the results reported by Endicott et al.[9b] The overall electrode process under these conditions at potentials where $[Co([14]aneN_4)(OH_2)_2]^{3+}$ is reduced but $[(Co([14]aneN_4)(OH_2))_2O_2]^{4+}$ and O_2 are not (e.g., −0.05 V) is the sum of reactions 1 and 2. Thus, one electron is consumed per molecule of cobalt(III) complex. The same is true in the absence of dioxygen and this explains why the total limiting current on the second plateau in curve 2 of Figure 7A matches the limiting current of curve 1. At potentials more negative than ca. −0.2 V $[(Co([14]aneN_4)(OH_2))_2O_2]^{4+}$ is reduced by another electron per cobalt with the release of hydrogen peroxide (curves 2 in Figure 7A and 7B):

$$[Co([14]aneN_4)(OH_2)_2]^{3+} + e \rightarrow [Co([14]aneN_4)(OH_2)_2]^{2+} \quad (1)$$

$$2[Co([14]aneN_4)(OH_2)_2]^{2+} + O_2 \rightarrow [(Co([14]aneN_4)(OH_2))_2O_2]^{4+} \quad (2)$$

$$[(Co([14]aneN_4)(OH_2))_2O_2]^{4+} + 2H^+ + 2e \rightarrow 2[Co([14]aneN_4)(OH_2)_2]^{2+} + H_2O_2 \quad (3)$$

Thus $[Co([14]aneN_4)(OH_2)_2]^{3+}$ acts as a catalyst for the reduction of dioxygen to hydrogen peroxide at potentials negative of ca. −0.2 V. Scheme I depicts the two-step process by which this catalysis proceeds. Our electrochemical measurements provided no direct evidence of the intermediacy of the superoxo complex, $[Co([14]aneN_4)(H_2O)_2]^{2+}$, shown in Scheme I but it is included on the basis of the spectral evidence given by Endicott et al.[9b]

Two additional features of Figure 7A require comment. On the basis of Scheme I one would expect the ring current shown in curve 4 of Figure 7A to reach the same limiting value as that in curve 3 because on the third plateau of curve 2 all of the cobalt(III) complex present is reduced to cobalt(II) at the disk and all of the dioxygen reaching the disk is converted to hydrogen peroxide. Similarly, the final limiting current of curve 5 would be expected to exceed that of curve 3 by the same factor that the limiting current of curve 2 exceeds that of curve 1. However, the limiting ring currents for curves 4 and 5 lie well below these expected values. This apparent discrepancy results in part from the reaction between the H_2O_2 and $[Co([14]aneN_4)(OH_2)_2]^{2+}$ generated at the disk during the time it takes them to reach the ring. A rate constant of 4×10^3 M^{-1} s^{-1} has been reported for this reaction.[23] (Note that this additional reaction proceeds too slowly to be important in solutions containing excess dioxygen.)

Scheme I

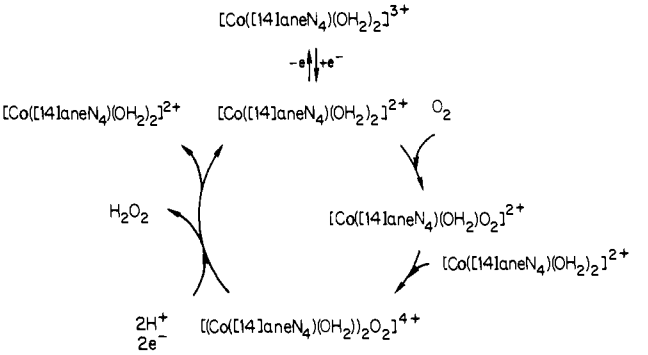

A second factor that also leads to the smaller ring currents can be discerned from curve 2 of Figure 7B: The disk potential is set at a value where only H_2O_2 and $[Co([14]aneN_4)(OH_2)_2]^{2+}$ are being produced at the disk, yet the wave at +1.1 in the ring current response shows that $[Co([14]aneN_4)(OH_2))_2O_2]^{4+}$ is nevertheless arriving at the ring. The μ-peroxocobalt(III)complex must be formed when the $[Co([14]aneN_4)(OH_2)_2]^{2+}$ departing from the outer edge of the disk encounters dioxygen in the gap between the disk and ring electrodes. The net result is that some of the cobalt(II) complex that would otherwise have reached the ring is converted into the μ-peroxocobalt(III) dimer. This accounts for the wave at 1.1 V in curve 2 of Figure 7B and contributes to the smaller ring currents in curves 4 and 5 of Figure 7A.

The formal potential of reaction 1 is 0.16 V vs. SSCE but in the presence of dioxygen the reduction proceeds at more positive potentials (Figures 3 and 7A) because $[Co([14]aneN_4)(OH_2)_2]^{2+}$ is rapidly scavenged by O_2. Reaction 3 exhibits a half-wave potential of −0.15 V at the disk electrode but the electrode process is irreversible. However, the formal potential for reaction 3 can be calculated from the standard potential of the O_2/H_2O_2 couple (0.44 vs. SSCE) and the equilibrium constant for reaction 4, which

$$[(Co([14]aneN_4)(OH_2))_2O_2]^{4+} + 2H_2O \rightleftarrows 2[Co([14]aneN_4)(OH_2)_2]^{2+} + O_2 \quad (4)$$

Endicott et al.[9b] report to be 1.7×10^{-10}. This leads to a calculated value of E^f for reaction 3 of 0.15 V vs. SSCE. The more negative potential required to cause reaction 3 to proceed at the rotating disk electrode (Figure 7A) reflects the existence of a kinetic barrier to the reduction that is commonplace in the electrochemistry of cobalt(III) complexes.[24]

The homogeneous reduction and oxidation of $[(Co([14]aneN_4)(OH_2))_2O_2]^{4+}$ by simple inorganic complexes have been studied recently by Wong and Endicott[22] who found that dissociation of the μ-peroxocobalt(III) complex into $[Co([14]aneN_4)(OH_2)O_2]^{2+}$ and $[Co([14]aneN_4)(OH_2)_2]^{2+}$ is the first and rate-limiting step for both reductions and oxidations. The rate constant governing the dissociation, ~ 0.6 s^{-1},[22] is much too small to be compatible with either of the steady-state limiting currents

(23) R. A. Heckman and J. H. Espenson. *Inorg. Chem.*, **18**. 38–43 (1979).
(24) N. Maki and N. Tanaka in "Encyclopedia of Electrochemistry of the Elements". Vol. III. A. J. Bard. Ed.. Marcel Dekker. Inc.. New York. 1975. Chapter 2.

Scheme II

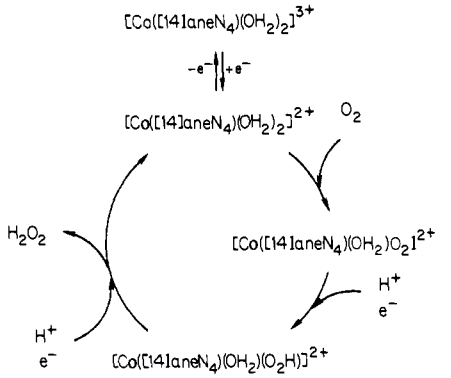

in curve 1 of Figure 8 for the reduction and oxidation of the μ-peroxocobalt(III) complex. Furthermore, the half-wave potential of the oxidation wave is very far removed from that of $[Co([14]aneN_4)(OH_2)_2]^{2+}$ (Table I) which is known to undergo reversible electrooxidation. Thus, the electrooxidation and -reduction of the μ-peroxocobalt(III) complex can be effected at suitable potentials by mechanisms that apparently do not involve dissociation of the complex as a prerequisite to reaction at the electrode.

Electrode Processes with Excess Dioxygen. The overall electrode process takes a different course when dioxygen is present in excess. The first reduction wave consumes two rather than one electron per cobalt(III) (figure 3) and neither hydrogen peroxide nor $[(Co([14]aneN_4)(OH_2))_2O_2]^{4+}$ is detected among the reaction products (Figure 5, curve 2). Only at potentials on the second reduction wave is hydrogen peroxide produced (Figure 5, curve 1). A reaction scheme to account for the observed behavior in the presence of excess dioxygen is shown in Scheme II.

The most important difference between Schemes I and II is the fate of the initial oxygen adduct formed from the reaction of $[Co([14]aneN_4)(OH_2)_2]^{2+}$ with O_2. With O_2 present in excess, the initial product is reduced at the electrode (Scheme II) rather than by reaction with a second molecule of $[Co([14]aneN_4)(OH_2)_2]^{2+}$ (Scheme I). This difference allows solutions of the two-electron reduction product to be generated by controlled potential reduction of $[Co([14]aneN_4)(OH_2)_2]^{3+}$ at its first reduction wave in the presence of excess dioxygen. Figure 6B shows the spectrum of the solution produced in this way. We believe the complex generated is the mononuclear hydroperoxide complex, $[Co([14]aneN_4)(OH_2)(O_2H)]^{2+}$. This complex is further reduced at more negative potentials in an irreversible process involving one electron per cobalt and leading to the release of H_2O_2 (Figure 3). The hydroperoxide complex also undergoes an irreversible oxidation at ca. 0.77 V (curve 2, Figure 5). We did not determine the products of this oxidation reaction but the ratio of ring to disk current for curve 2 of Figure 5 is about the same as would be obtained if O_2 were being reduced to H_2O_2 at the disk and the H_2O_2 were being re-oxidized at the ring. We therefore assume that the oxidation of $[Co([14]aneN_4)(OH_2)(O_2H)]^{2+}$ produces O_2 and $[Co([14]aneN_4)(OH_2)_2]^{3+}$. In any case, the oxidation wave at 0.77 V serves to distinguish $[Co([14]aneN_4)(H_2O)(O_2H)]^{2+}$ from H_2O_2 which is not oxidized until +0.9 V.

The second reduction step in Scheme II, reaction 5, must have

$$[Co([14]aneN_4)(H_2O)O_2]^{2+} + H^+ + e^- \rightarrow [Co([14]aneN_4)(H_2O)(O_2H)]^{2+} \quad (5)$$

a formal potential that is considerably more positive than that of the $[Co([14]aneN_4)(OH_2)_2]^{3+/2+}$ couple (0.16 vs. SSCE). This follows from the experiments of Endicott et al.,[9b] who observed a transient intermediate that they identified as $[Co([14]aneN_4)(OH_2)O_2]^{2+}$ which was rapidly reduced by reaction with $[Co([14]aneN_4)(OH_2)_2]^{2+}$. The immeasurably rapid rate of reaction 5 at the graphite disk electrode at potentials as positive as 0.25 V (Figure 3) also signals a formal potential for reaction 5 that lies at considerably more positive potentials. Endicott et al. compared the mean stability per cobalt of the coordination of O_2^- and O_2^{2-} to the cobalt(III) centers in $[Co([14]aneN_4)(OH_2)O_2]^{2+}$ and $[(Co([14]aneN_4)(H_2O))_2O_2]^{4+}$, respectively.[9b] Surprisingly, they found that the binding energies do not differ substantially despite the large differences in the basicities of the two ligands. If the binding energies of O_2^- and O_2H^- in the two cobalt complexes in reaction 5 were also comparable, the formal potential of reaction 5 would be equal to that for reaction 6, which

$$O_2^- + H^+ + e^- = HO_2^- \quad (6)$$

can be calculated to be 0.76 V vs. SSCE from the data given by Ilan et al.[25] Thus, several lines of evidence point to a formal potential for reaction 5 that is significantly positive of 0.25 V.

Of the three, successive, one-electron reductions in Scheme II that comprise the catalyzed reaction of O_2 to H_2O_2, the final step, reaction 7, limits the potential at which the catalyzed reduction

$$[Co([14]aneN_4)(OH_2)(O_2H)]^{2+} + e^- + H^+ \rightarrow [Co([14]aneN_4)(OH_2)_2]^{2+} + H_2O_2 \quad (7)$$

can be carried out. Unless the potential is made negative enough for reaction 7 to proceed the reduction of oxygen ceases because the catalyst is trapped as $[Co([14]aneN_4)(OH_2)(O_2H)]^{2+}$. Unfortunately, reaction 7 proceeds irreversibly at the electrode and the datum needed for a calculation of the formal potential of the reaction (i.e., the equilibrium constant for the coordination of HO_2^- to $[Co([14]aneN_4)(OH_2)_2]^{3+}$) is not available. Nevertheless, it is clear in general that the formal potentials of catalysts measured in the absence of the substrates whose reductions (or oxidations) it is desired to catalyze may lie far from the potential where the catalysis actually proceeds, especially when intermediates less reactive than the initial catalyst are involved.

Possible Structure of $[Co([14]aneN_4)(OH_2)(O_2H)]^{2+}$. The structure of the product formed when $[Co([14]aneN_4)(OH_2)_2]^{3+}$ is reduced at ca. 0 V in the presence of excess dioxygen (Figure 3, curve 2) is of interest. The electrochemical data show that two electrons per cobalt(III) are consumed in its formation and its electronic spectrum exhibits an intense shoulder at 300 nm that is consistent with a charge-transfer transition involving peroxide coordinated to cobalt(III).[26,27] Either "end-on" or "side-on" bonding seems possible since examples of both types are known in cobalt(III)–peroxo complexes.[26,27] If "side-on" bonding were

Table II. UV-vis Spectral Data

complex	λ_{max}, nm	ϵ, M^{-1} cm^{-1}	ref
trans-$[Co([14]aneN_4)(OH_2)_2]^{3+}$	242	14000	this work
	428	54	(0.5 M $HClO_4$)
	570	32	
$[(Co([14]aneN_4)(OH_2))_2O_2]^{4+}$	227	30000	this work
	300 sh	9600	(0.5 M $HClO_4$)
	428	410	
	548	120	
$[Co([14]aneN_4)(OH_2)(O_2H)]^{2+}$	225	16000	this work
	300 sh	3500	(0.5 M $HClO_4$)
	522	43	
	616	40	
cis-$[Co([14]aneN_4)(OH_2)_2]^{3+}$	367	99	29
	506	110	
cis-$[Co([14]aneN_4)(CO_3)]^+$	365	140	28
	520	154	
$[Co(2{=}phos)_2O_2]^{+a}$	322	17800	27
	385	1200	
	462	1170	
	620 sh	16	
$[Co(2{=}phos)_2CO_3]^{+a}$	487	1630	

[a] 2=phos is *cis*-1,2-*bis*(diphenylphosphino)ethylene.

(25) Y. A. Ilan, G. Zapski, and D. Meisel, *Biochem. Biophys. Acta*, **430**, 209–215 (1976).
(26) L. Vaska, *Acc. Chem. Res.*, **9**, 175–183 (1976).

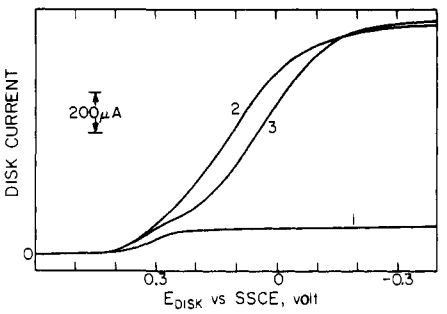

Figure 9. Rotating disk current-potential curve for 0.9 mM $[Co(Me_6[14]4,11\text{-diene } N_4)(OH_2)_2]^{3+}$ recorded at a rotation rate of 900 rpm. Supporting electrolyte: (curve 1) 0.5 $MHClO_4$, deaerated, (curve 2) 0.5 M $HClO_4$, saturated with dioxygen, and (curve 3) 0.1 M $HClO_4$, saturated with dioxygen.

present the macrocyclic ligand would presumably have rearranged to provide coordination sites for a cis configuration of the coordinated peroxo group. UV and visible spectra of several complexes of known structure are listed along with that of $[Co([14]aneN_4)(OH_2)(O_2H)]^{2+}$ in Table II. If the latter contained side-bonded peroxide one might expect its spectrum to have some features in common with those of the *cis*-1,2-*bis*(diphenylphosphino)ethylenecobalt(III),[28] *cis*-$[Co([14]aneN_4)(CO_3)]^+$,[29] or *cis*-$[Co([14]aneN_4)(OH_2)_2]^{3+}$ complexes.[30] However, the ligand field transitions observed in the spectra of the *cis*-$[14]aneN_4$) complexes have little in common with the spectrum in Figure 6B. Instead, this spectrum resembles much more that of $[(Co([14]aneN_4)(OH_2))_2O_2]^{4+}$ which is believed to contain a bridging, end-bonded peroxo ligand.[11] The coordination of cobalt(III) to one of the oxygen atoms in a peroxo ligand is not likely to decrease the basicity of the other oxygen sufficiently for it to remain unprotonated in acidic electrolytes. Thus, we have chosen to write the complex as an end-bonded hydroperoxide complex, *trans*-$[Co([14]aneN_4)(OH_2)(O_2H)]^{2+}$. If this interpretation is correct, the complex is an example of a stable, nonbridging, hydroperoxo complex of cobalt(III), a class of complexes which has only recently been encountered.[22]

Rate of Reaction of $[(Co([14]aneN_4)(OH_2)_2]^{2+}$ with O_2. The rate constant reported by Endicott et al.[9b] for the reaction of $[Co([14]aneN_4)(OH_2)_2]^{2+}$ with O_2, $k_{O_2} = 5 \times 10^5$ M^{-1} s^{-1}, is consistent with our observations that none of the reduced complex could be detected at the ring electrode in air-saturated solutions at the highest accessible rotation rates. With a rate constant this large it would be necessary to employ reactant concentrations in the micromolar range in order to be able to observe the oxidation of $[Co([14]aneN_4)(OH_2)_2]^{2+}$ at the ring electrode[31] and experiments at such low concentrations produced currents that were too small for reliable measurement with the ring–disk electrode. Our results show that none of the steps in Scheme II subsequent to the reaction between $[Co([14]aneN_4)(OH_2)_2]^{2+}$ and O_2 proceed more slowly than this initial reaction when the electrode potential is fixed on the plateau of the second wave in Figure 3.

Behavior of a Related Macrocyclic Complex. The general features of the mechanistic pattern depicted in Scheme II might well apply to other macrocyclic complexes of Co(III) but differences in reaction rates and reduction potentials would be expected.[32] We examined briefly the electrochemical response of the $[Co(Me_6[14]4,11\text{-dieneN}_4)(OH_2)_2]^{3+}$ complex[33,34] at the rotating disk electrode and recorded the curves shown in Figure 9. The complex proved to be an even better catalyst for the reduction of O_2 to H_2O_2 in the sense that the catalyzed reduction proceeded at potentials ca. 300 mV more positive than was true for $[Co([14]aneN_4)(OH_2)_2]^{3+}$. The rate of the catalyzed reaction is lower, however, since the reduced catalyst could be detected at the ring electrode under the same conditions where no ring current was observed for $[Co([14]aneN_4)(OH_2)_2]^{2+}$. Two waves are evident at pH 1 with magnitudes that are roughly compatible with what would be expected if Scheme II applied to this complex as well. As the pH is lowered the second wave shifts to more positive potentials (just as was true of the second wave in Figure 3) until a single, composite wave results that corresponds to the direct catalyzed reduction of O_2 to H_2O_2 at a potential only ca. 300 mV less positive than the reversible potential for this reaction (i.e., 0.4 V vs. SSCE in 0.5 M H^+).

We are continuing studies with this and related complexes to determine if changes in the degree of unsaturation in the macrocyclic ligand and in the nature of the axial ligands[8] may lead to a catalyst that functions even closer to the reversible potential for the reduction of O_2 to H_2O_2.

Concluding Comments. One of the reasons for undertaking this study was the hope that the electrochemical behavior of the dioxygen adducts of the cobalt complex encountered might provide insight into the mechanism by which the recently described cofacial dicobalt porphyrin catalyst functions.[5] When adsorbed on graphite electrodes this catalyst achieves the four-electron reduction of dioxygen without the detectable intermediacy of hydrogen peroxide but the cobalt–dioxygen adducts that presumably participate in the catalysis[5] have yet to be detected.

The results of the present study have shown that coordinating a macrocyclic cobalt(III) complex to both ends of a peroxide dianion is not sufficient to activate it toward reduction. Under no conditions did we detect any reduction of the bridging peroxide group in the μ-peroxocobalt(III) dimer. Attempts to do so by making the electrode potential more negative led only to the reduction of the cobalt(III) centers and the release of hydrogen peroxide. The greater degree of unsaturation and, especially, the bridging links that constrain the two macrocyclic rings in the more active, dimeric cobalt(II) porphyrin catalysts (5) would appear to be crucial. We intend to explore the relative importance of these two factors in continuing studies of the reactions of dioxygen with macrocyclic cobalt(II) complexes of increasingly unsaturated ligands.

Acknowledgment. This work originated as part of a collaborative effort in which the research groups of Professors M. Boudart, J. P. Collman, and H. Taube (Stanford University) and H. Tennent (Hercules, Inc. Research Center) were involved. Stimulating discussions and helpful suggestions from several members of these groups are a pleasure to acknowledge. We thank Profesor John Endicott for sending us copies of manuscripts prior to publication and for helpful general information on the chemistry of the complexes studied. The work was supported by the National Science Foundation.

(27) A. B. P. Lever and H. B. Gray, *Acc. Chem. Res.*, **11**, 348–355 (1978).
(28) V. M. Miskowski, J. L. Robbins, G. S. Hammond, and H. B. Gray, *J. Am. Chem. Soc.*, **98**, 2477–2483 (1976).
(29) Y. Hung, L. Y. Martin, S. C. Jackels, A. M. Tait, and D. H. Busch, *J. Am. Chem. Soc.*, **99**, 4029–4039 (1977).
(30) C. K. Poon and M. L. Tobe, *J. Chem. Soc. A*, 1549–1555 (1968).
(31) K. B. Prater and A. J. Bard, *J. Electrochem. Soc.*, **117**, 1517–1520 (1970).
(32) R. D. Jones, D. A. Summerville, and F. Basolo, *Chem. Rev.*, **79**, 139–173 (1979).
(33) N. Sadasivan, J. A. Kernohan, and J. F. Endicott, *Inorg. Chem.*, **6**, 770–780 (1967).
(34) We thank W. R. Pangratz for the sample of this complex.